

Article

The Role of Drying Schedule and Conditioning in Moisture Uniformity in Wood: A Machine Learning Approach

Sohrab Rahimi ^{1,2}, Vahid Nasir ^{1,3,*}, Stavros Avramidis ¹ and Farrokh Sassani ³¹ Department of Wood Science, University of British Columbia, Vancouver, BC V6T 1Z4, Canada² FPInnovations, Vancouver, BC V6T 1Z4, Canada³ Department of Mechanical Engineering, University of British Columbia, Vancouver, BC V6T 1Z4, Canada

* Correspondence: vahid.nasir@ubc.ca

Abstract: Monitoring the moisture content (MC) of wood and avoiding large MC variation is a crucial task as a large moisture spread after drying significantly devalues the product, especially in species with high green MC spread. Therefore, this research aims to optimize kiln-drying and provides a predictive approach to estimate and classify target timber moisture, using a gradient-boosting machine learning model. Inputs include three wood attributes (initial moisture, initial weight, and basic density) and three drying parameters (schedule, conditioning, and post-storage). Results show that initial weight has the highest correlation with the final moisture and possesses the highest relative importance in both predictive and classifier models. This model demonstrated a drop in training accuracy after removing schedule, conditioning, and post-storage from inputs, emphasizing that the drying parameters are significant in the robustness of the model. However, the regression-based model failed to satisfactorily predict the moisture after kiln-drying. In contrast, the classifying model is capable of classifying dried wood into acceptable, over-, and under-dried groups, which could apply to timber pre- and post-sorting. Overall, the gradient-boosting model successfully classified the moisture in kiln-dried western hemlock timber.

Keywords: western hemlock; wood moisture; drying schedule; conditioning; TreeNet gradient-boosting; machine learning; ensemble learning



Citation: Rahimi, S.; Nasir, V.; Avramidis, S.; Sassani, F. The Role of Drying Schedule and Conditioning in Moisture Uniformity in Wood: A Machine Learning Approach. *Polymers* **2023**, *15*, 792. <https://doi.org/10.3390/polym15040792>

Academic Editor: Antonios Papadopoulos

Received: 12 January 2023

Revised: 30 January 2023

Accepted: 2 February 2023

Published: 4 February 2023



Copyright: © 2023 by the authors. Licensee MDPI, Basel, Switzerland. This article is an open access article distributed under the terms and conditions of the Creative Commons Attribution (CC BY) license (<https://creativecommons.org/licenses/by/4.0/>).

1. Introduction

Timber drying impacts the final product quality and plays an essential role in the dimensional stability, and mechanical properties of timber, as the physical [1], elastic and viscoelastic properties of wood are moisture-dependent [2]. Additionally, timber drying facilitates coating, cutting, and remanufacturing procedures, rendering dried wood less susceptible to deformation, cracks, and decay [3,4]. Target moisture (M_t) in kiln-drying should correspond to the indoor or outdoor environment where the final product will be used. A well-managed drying operation dramatically improves timber drying quality [5,6].

Considerable variability in initial moisture (M_i) among timber pieces of the same kiln batch is inevitable, especially in softwoods with substantial differences between the properties of sapwood and heartwood [7]. Different timber pieces in the same load undergo various drying levels due to inherent variations in M_i and other wood properties [8,9]. Consequently, final moisture (M_f) among timber fluctuates along a broad range. Large-scale kilns aggravate this problem because of the non-uniform kiln-drying conditions in the chamber's width, depth, and height [10]. Non-uniformity of the final moisture between kiln-dried timber pieces substantially impacts their monetary values. Over-dried wood is in less demand in the market since over-drying increases shrinkage and shapes distortion [11]. Additionally, under-dried wood is hardly acceptable in the market due to its susceptibility to fungal decay and low mechanical strength [11].

Almost every wood species requires a specific drying schedule, which could be time-based, moisture-based, or combined [12]. Drying schedules involve predetermined heat,

humidification, ventilation, and air circulation [13,14]. Combined (time- and moisture-based) schedules typically apply to the kiln-drying coastal softwood species in British Columbia, Canada. In a combined schedule, drying factors are time-based from the beginning of the drying until around the fiber saturation point (M_{fsp}). However, upon reaching that point, they become constant until reaching M_t . Drying schedules' aggressiveness influences the final moisture variation in a kiln batch [8,15]. Moreover, post-drying steps such as conditioning in kilns and outdoor storage may apply to reduce moisture variation within and between timber pieces [16,17]. Conditioning is a high-humidity step at the end of some drying schedules (after reaching M_t) to minimize the moisture differences between and within timber pieces (shell and core of timber) and relieve internal stresses (casehardening) [9]. However, some Japanese sawmills use stickers and store kiln-dried batches outdoors for a period of one to two weeks to reduce the moisture variation and moisture profile in thickness, resulting in internal stress dissipation [16].

Pacific coast hemlock (also known as "hem-fir") is an abundant source of fiber on the British Columbia coast which is comprised of western hemlock (*Tsuga heterophylla*) and amabilis fir (*Abies amabilis*) [18]. Thick solid hem-fir products, specifically timbers with cross-sectional areas of $90 \times 90 \text{ mm}^2$, $105 \times 105 \text{ mm}^2$, and $115 \times 115 \text{ mm}^2$ (also known as "baby-squares") are commonly the preferred material in timber construction, especially in Japan, which is one of BC's largest overseas markets [19]. Hemlock is a difficult-to-dry species due to its naturally high green moisture content, the presence of wet wood (or wet pockets), and often compression wood. Past research focused on optimizing drying schedules [15,20,21], pre-sorting [22–24], and post-sorting [25] strategies. Studies examining the collapse and recovery during the drying process [26,27], cracking occurrence during the drying process [28], and numerical simulations of coupled moisture and heat transfer in wood during kiln drying [29] were also reported in the literature. Kiln-drying scheduling is also covered in some studies [30,31] as an important factor impacting the final moisture content and drying defects [32]. In addition, previous studies focused on characterizing and modeling final moisture and its spread in air-dried [33], radio-frequency kiln-dried [34–36], heat treated [37], and heat-and-vent kiln-dried batches [38–40]. Additionally, previous studies investigated moisture prediction in kiln-dried lumber merely based on wood properties; however, the combined effects of drying conditions and wood properties on the moisture uniformity after kiln-drying still represent a knowledge gap [41]. Furthermore, initial wood indices, especially M_i content and its variation, remarkably affect M_f variation. Therefore, a holistic approach is required to characterize the combined effects of wood indices and drying schedules on wood properties after kiln-drying [38]. For this reason, the current study aims to investigate and predict the M_f of kiln baby-square western hemlock under different schedules.

Accordingly, a machine learning approach was adopted to study the relationship between the wood properties and to quantify the roles of drying schedule, conditioning, and post-storage. This study uses a gradient-boosting algorithm known as TreeNet for moisture prediction and classification. The most widely used machine learning models in the literature on wood science and technology are artificial neural networks (ANNs). They have been used in a wide range of applications for wood identification [42,43], defect detection [42,43], and wood properties prediction [44,45]. The most emphases were on employing the multilayer perceptron (MLP) model [46–48]. However, compared to ANNs, fewer studies investigated the performance of ensemble machine learning methods such as gradient boosting for predicting wood properties. Ensemble learning improves prediction accuracy by using multiple machine learning algorithms known as a weak learner and fusing the results by applying a different voting mechanism [49]. This study uses the TreeNet gradient boosting model, variable clustering, and correlation analysis to predict the M_f in kiln-dried western hemlock and explain the role of initial wood properties, drying schedules, and conditioning on the moisture distribution in dried timber.

2. Materials and Methods

2.1. Materials

A local sawmill located on Vancouver Island, British Columbia provided 96 timber pieces of second-growth western hemlock baby squares (116 mm × 116 mm; 3.96 m in length) for this study. All timber pieces were in green condition with a grade of II (standard) or better [50]. Each piece was cut into four kiln specimens and five cookies using a circular saw. Figure 1 represents the cutting protocol. According to the cutting protocol, one section of 100 mm in length was removed from each end of every timber piece to mitigate the risk of end moisture loss. Subsequently, four kiln specimens and five cookies were cut from each timber piece. The length of the kiln specimens and cookies were 900 mm and 25 mm, respectively. Overall, 480 cookies and 384 kiln specimens were provided from the entire timber population.

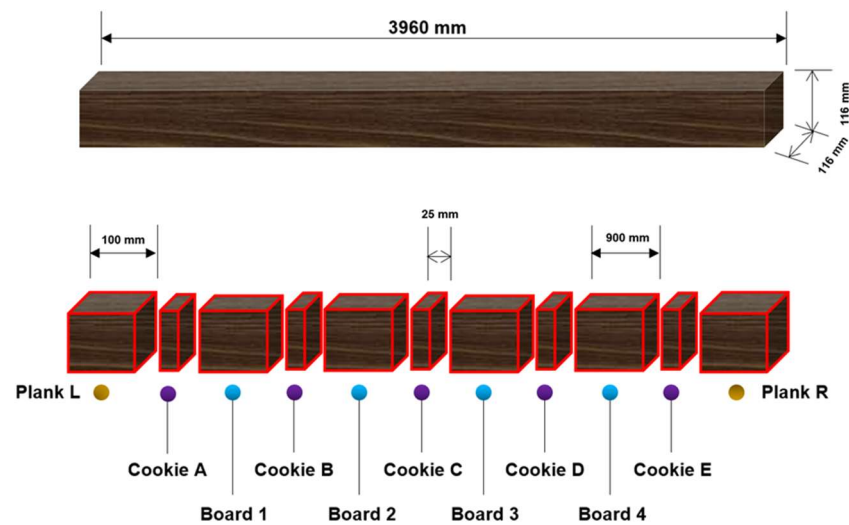


Figure 1. Cutting pattern of the baby-square western hemlock.

2.2. Experiments

Cookies were used to measure M_i and basic density (ρ_b) according to Kollmann [51] and Skaar [52]. In the next step, six out of 384 kiln specimens were arbitrarily discarded, and the rest (378 kiln specimens) were randomly assigned to nine drying batches. Table 1 summarizes the nine drying runs used in this study. The control drying schedule was applied to the first drying batch, followed by conditioning. The first modified drying schedule had four modes as the combination of presence and absence of conditioning and post-storage. Similarly, the second modified drying schedule had four modes as the combination of existence and nonexistence of conditioning and post-storage.

Table 1. Nine drying batches of baby square western hemlock.

Run Number	Schedule	Conditioning	Storage	Name
1	Control (unmodified)	Yes	No	UN
2	Modified I	Yes	No	I_C_NS
3	Modified I	No	No	I_NC_NS
4	Modified II	No	No	II_NC_NS
5	Modified I	Yes	Yes	I_C_S
6	Modified I	No	Yes	I_NC_S
7	Modified II	Yes	Yes	II_C_S
8	Modified II	No	Yes	II_NC_S
9	Modified II	Yes	No	II_C_NS

Each drying batch contained 42 timber specimens. The M_i and ρ_b could influence the M_f and needed to be neutralized to make the drying results comparable between all drying batches. Therefore, the entire timber population was categorized into nine groups so that M_i and ρ_b had the smallest standard deviation. The cross-sections of the specimens were coated using polyvinyl acetate (PVA) before drying to prevent end moisture loss. A conventional heat-and-vent kiln with a capacity of 0.73 m³ in FPIInnovations, Vancouver, British Columbia was used for this research. The same aluminum stickers, with a weight and length of 8.94 kg and 19 mm, respectively, were used for each drying run, which contained 42 kiln specimens (six rows and seven columns).

The drying schedule developed in the past [53,54] was used as the control (unmodified) schedule. This time-based schedule consisted of eight steps, using a pre-determined number of hours for each step. In step nine, the drying process was switched to a moisture content-based schedule, drying the timber to the M_t without changing the settings. The M_t was set to 12%, the average equilibrium moisture content M_{emc} in Japan from October to May [16]. This M_t was chosen to avoid additional moisture loss from the specimens during post-drying storage time. The last step (conditioning) was time-based. After completing a drying run, the timber pieces cooled down for twelve hours inside the kiln with the doors closed. In addition to the control schedule, two modified drying schedules were also used. In schedule I, the same dry-bulb temperature was reached in the last step and the M_{emc} decreased more aggressively. Schedule II was considered an aggressive drying schedule because it reached a higher dry-bulb temperature in the final drying step, having a steep reduction in M_{emc} . Furthermore, the M_f was kept under 93 °C to avoid developing a honeycomb. Tables 2–4 illustrate the control schedule, schedule I, and schedule II, respectively. All kiln specimens were reweighed post-drying to evaluate their final moisture M_f .

Table 2. Control (unmodified) drying schedule used in industrial kilns in British Columbia sawmills. This schedule comprises eight time-based steps, one moisture-based step, and one conditioning step.

Step	Time (h)	Dry-Bulb Temperature (°C)	Wet-Bulb Temperature (°C)	Relative Humidity (%)	Equilibrium Moisture Content (%)
1	12	48.9	48.9	100.0	25.5
2	24	51.7	50.6	94.2	20.8
3	24	55.0	52.8	89.0	17.6
4	24	57.8	55.0	86.5	16.2
5	24	61.7	56.7	77.7	12.7
6	24	65.6	58.9	71.9	10.8
7	24	70.0	60.6	63.7	8.8
8	24	73.9	62.8	59.4	7.8
9	Till $M_f = 12\%$	77.8	65.0	55.7	7.0
10	12	71.7	66.7	79.4	12.3

Table 3. First modified schedule. This schedule comprises six time-based steps and one moisture-based step, followed by optional conditioning (step 8) and optional post-storage (step 9).

Step	Time (h)	Dry-Bulb Temperature (°C)	Wet-Bulb Temperature (°C)	Relative Humidity (%)	Equilibrium Moisture Content (%)
1	12	48.9	48.9	100.0	25.5
2	24	57.8	54.4	83.8	15.1
3	24	54.4	46.1	62.7	9.7
4	24	60.0	46.1	46.1	6.8
5	24	62.2	46.1	41.0	6.0
6	24	71.1	51.7	37.0	5.1
7	Till $M_f = 12\%$	78.8	54.4	30.1	4.1
8	12 (optional)	71.7	66.7	79.4	12.3
9	168 (optional)	20	16	65	12.3

Table 4. Second modified schedule. This schedule comprises five time-based steps and one moisture-based step, followed by optional conditioning (step 7) and optional post-storage (step 8).

Step	Time (h)	Dry-Bulb Temperature (°C)	Wet-Bulb Temperature (°C)	Relative Humidity (%)	Equilibrium Moisture Content (%)
1	12	48.9	48.9	100.0	25.5
2	24	62.8	60.6	89.8	17.2
3	24	68.3	64.4	83.2	13.9
4	24	71.1	64.4	73.1	10.7
5	24	79.4	64.4	50.4	6.2
6	Till $M_f = 12\%$	85.0	64.4	39.5	4.7
7	12 (optional)	71.7	66.7	79.4	12.3
8	168 (optional)	20	16	65	12.3

After kiln-drying, all timber pieces were reweighed. The kiln-dried weight or final weight (w_f) of each sample was used to calculate its M_f , according to the equations documented in Perre [8] and Siau [55].

2.3. Machine Learning

The model inputs included M_i , w_i , ρ_b , types of drying schedule (control, I, II), conditioning (Yes/No), and post-drying storage (Yes/No). The objective was to predict the M_f and classify the timber condition after drying. Accordingly, the boards with $M_f < 10$ and $M_f \geq 19$ were labeled as over-dried and under-dried, respectively. Additionally, boards with $10 \leq M_f < 19$ were labeled as normal. TreeNet, a gradient-boosting algorithm, was used for both the regression and classification tasks. It uses the decision tree-based CART model [56] for ensemble learning. Decision tree models are easy to interpret, and the importance of the predictor variables and their relationships can be identified through exploratory data analysis. Details of the CART model can be found elsewhere [57,58]. The CART algorithm was successfully used for check prediction in weathered thermally modified timber [59] and for characterization and classification of artificially weathered wood [60–62]. Ensemble learning based on bagging or boosting algorithms could be applied to reduce the variance of a single prediction by a tree using multiple weak learners (decision tree). A benchmark study on medium-sized data has shown that tree-based ensemble models such as XGBoost (eXtreme Gradient Boosting) and random forest could outperform the ANNs despite the presence of irregular patterns in the target function and uninformative features [63]. Random forest uses the bagging method, in which each tree is trained using a subset of data, and the model output is based on the voting scheme among weak learners [64]. Random forest was used to predict the mechanical properties of wood fiber insulation boards [65]. It is also utilized in wood machining for tool temperature prediction [66] and frozen lumber classification [67].

Unlike bagging methods, in which weak learners are trained in a similar way, boosting methods perform the training process sequentially, whereas subsequent models correct the performance of prior models. In the gradient-boosting algorithm of TreeNet, a subset of data is used to train a CART model with a maximum number of terminal nodes or tree depth. Then, the CART model is updated depending on the loss function but shrinks the update by the defined learning rate. The process is repeated, and CART models are sequentially added for a specified number of iterations, equal to the number of trees to build [68]. Boosting methods are used for wood species recognition [69], online color classification systems of solid wood flooring [70], predicting the mechanical properties of wood composite [71], and wood machining monitoring [72]. In this study, the number of trees was set to 2000. Additionally, the maximum terminal node per tree and the minimum number of cases allowed for a tree were set to 12 and 3, respectively. Additionally, the learning rate and subsample fraction were equal to 0.01 and 0.3, respectively. Finally, the

number of predictors for node splitting was equal to the square root of the total number of predictors.

3. Results and Discussion

The results will analyze and characterize the selected initial and final wood indices and their correlation with drying parameters, drying schedule aggressiveness, drying condition, and post-drying storage. Then, a predictive approach will be provided to estimate the M_f of each timber piece based on its corresponding wood properties and drying conditions. Finally, a classification approach will be delivered to categorize dried wood into three groups: Acceptable (normal), over-dried, and under-dried.

3.1. Wood Indices and Drying Parameters Analysis

Figures 2 and 3 are interval plots representing the impact of conditioning and post-storage on the M_f variation, respectively. These results are based on the 95% of confidence interval for the M_f mean. Both figures indicate that modified drying schedules considerably increased the average M_f , and this effect is more noticeable than the conditioning or post-storage. The control drying schedule had eight time-based steps that took 180 h, which was longer than the modified drying schedules. This long drying time gives grounds to the lower M_f mean at the end of the control drying run, as it allocated sufficient time for under-dried wood to decrease in moisture. Applying conditioning and post-storage reduced the variation in M_f for both modified schedules because, while conditioning and post-storage allow under-dried wood to lose moisture, they let over-dried wood regain moisture. Additionally, while for each drying schedule the role of conditioning and post-storage is insignificant, there was a remarkable difference between the M_f in the two modified drying schedules when the timber pieces underwent conditioning or post-storage.

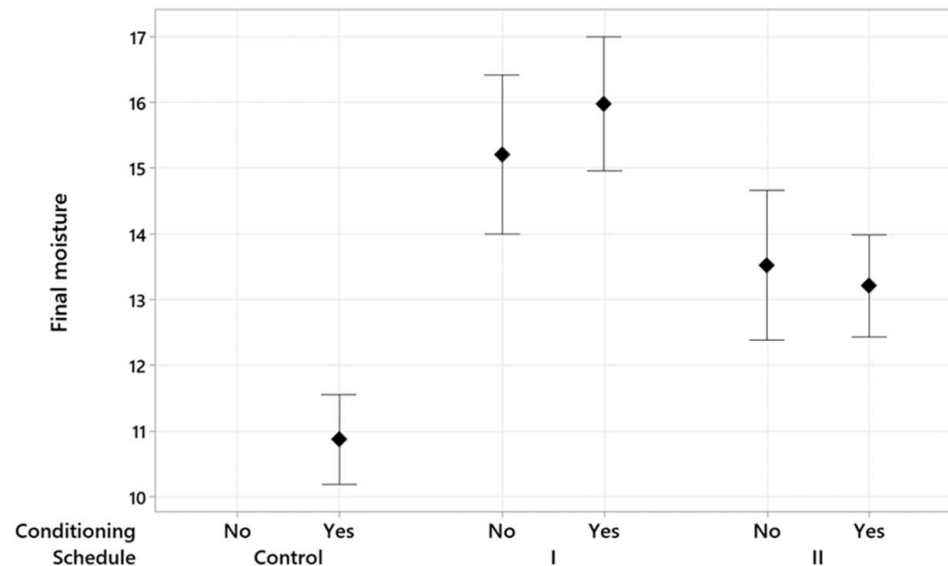


Figure 2. Interval plot of the M_f for different drying schedules with the presence and absence of conditioning treatment. The results are at 95% of the confidence interval for the M_f mean.

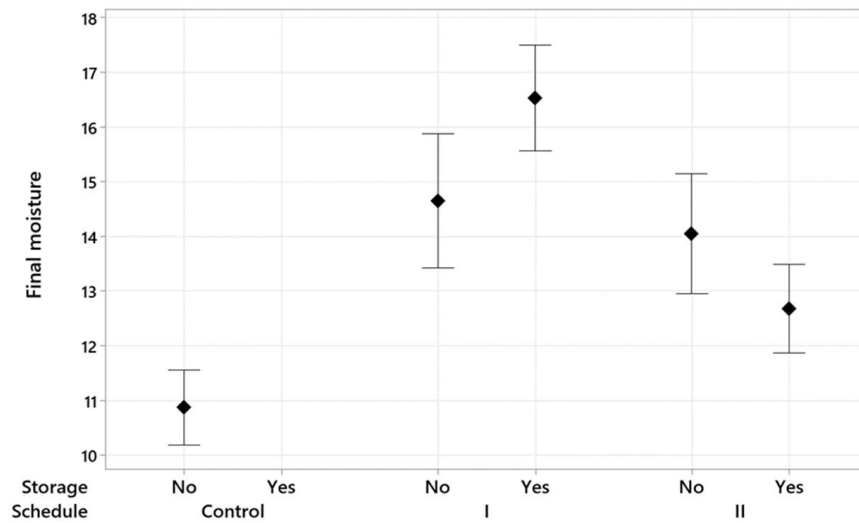


Figure 3. Interval plot of the M_f for different drying schedules with the presence and absence of post-storage treatment. The results are at 95% of the confidence interval for the M_f mean.

Figures 4–6 are three histograms depicting the distribution of M_f . Figure 4 shows that schedule I accounts for the highest M_f mean (15.59%) and variation (5.16%), while the lowest M_f mean (10.87) and variation (2.19) values belong to the 42 timber pieces that underwent the control schedule. The M_f mean is very close to the M_t , which could be attributed to the long drying time compared to the modified ones. Figure 5 demonstrates that timber pieces with conditioning had a slightly smaller standard deviation (4.31%) than those without conditioning (StDev = 5.47%). Likewise, Figure 6 exhibits that timber pieces with post-storage had an insubstantial smaller standard deviation (4.54%) than those without conditioning (StDev = 5.07%). In conditioning and post-storage, the M_{emc} (12.3%) is very close to M_t (12%), letting the M_f reach M_t and increasing moisture uniformity.

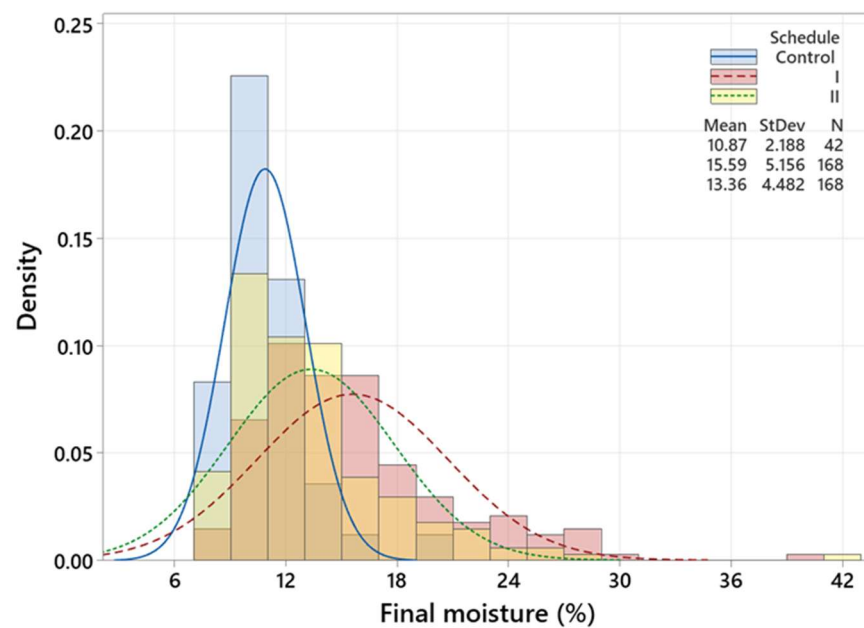


Figure 4. Histogram and distribution curves of the M_f for the control, modified I and modified II schedules.

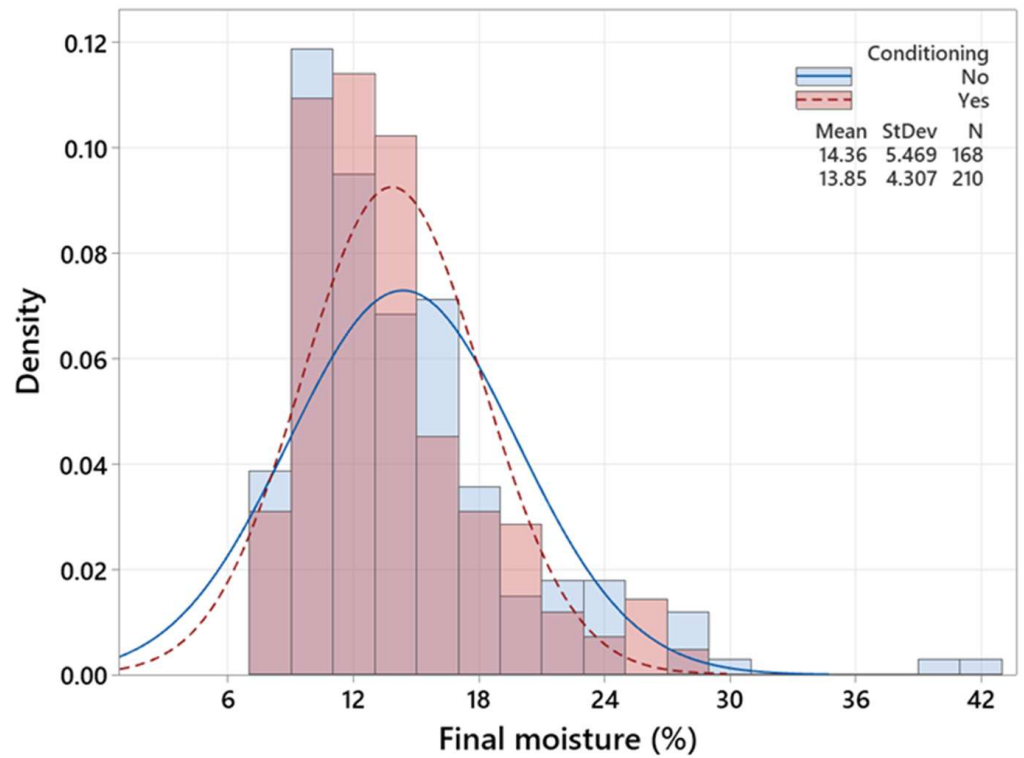


Figure 5. Histogram and distribution curves of the M_f in the existence and nonexistence of the conditioning treatment.

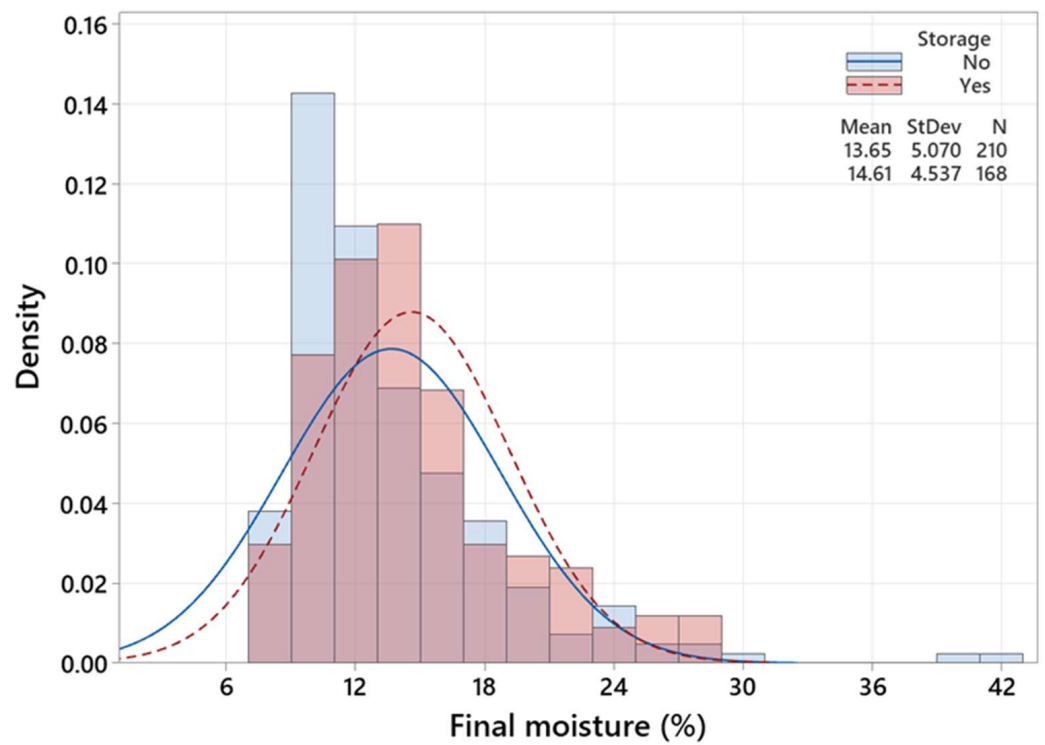


Figure 6. Histogram and distribution curves of the M_f in the existence and nonexistence of the post-storage treatment.

The dependency between the w_i and M_i , M_f , and ρ_b could be studied through a hierarchical clustering analysis, as explained by Fathi et al. [73]. The dendrogram (Figure 7) demonstrates three clusters and shows the similarity level between the studied variables. This dendrogram indicates that ρ_b had the smallest similarity value (45.42%) with the M_f , which accords with the findings of the previous research on 2" × 4" hem-fir [38]. In the present study, M_i and w_i showed the most similarity, while Rahimi and Avramidis [38] observed the most similarity between M_f and M_i in the previous research. The initial weight of the timber can be measured accurately and non-destructively. It is challenging to measure the moisture above the fiber saturation by moisture meters, and cutting cookies is a time-consuming and destructive method that cannot be performed at sawmills.

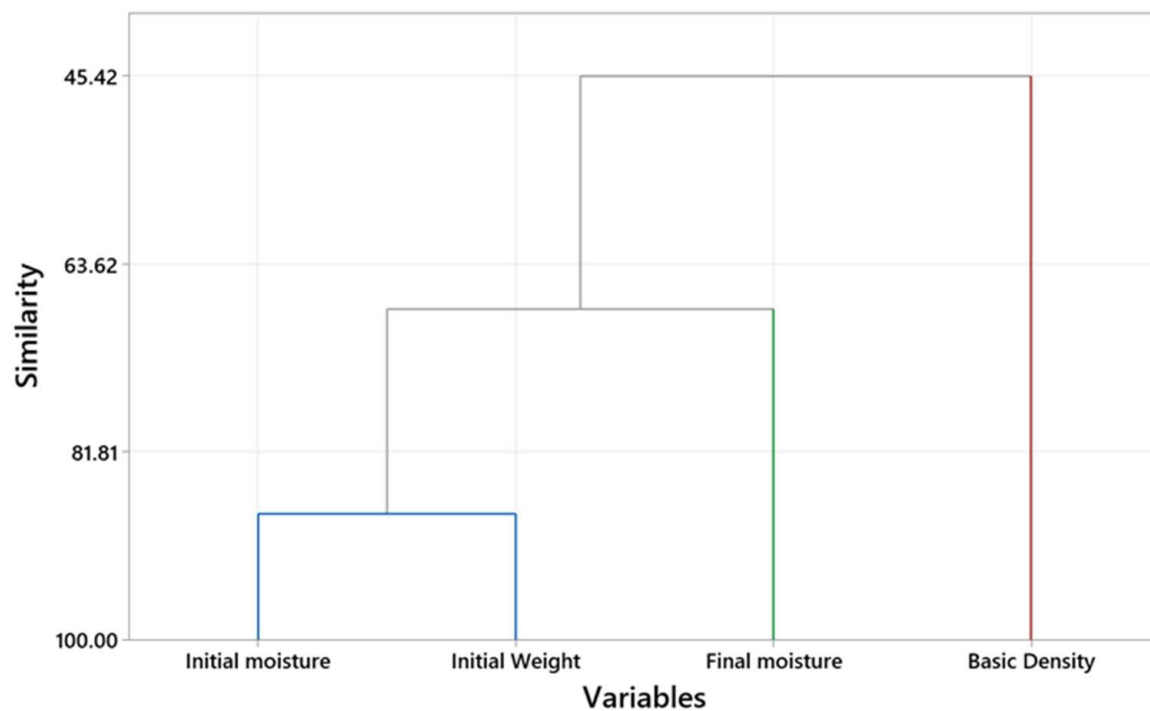


Figure 7. The variable clustering analysis illustrates the correlation coefficient distance between wood attributes.

It was interesting to see that the drying schedule, conditioning, and post-storage protocols noticeably impacted the correlation between the M_f and the input variables. Table 5 documents the correlation between M_f and initial wood indices in nine drying runs. Accordingly, the highest correlation between M_i and M_f (0.62%) was in I_C_NS (abbreviated names defined in Table 1), while the lowest correlation between M_i and M_f (0.15%) was in UN. Furthermore, the highest correlation between ρ_b and M_f (0.60%) was in II_NC_NS, while the lowest correlation between ρ_b and M_f (0.12%) was in II_NC_S. Moreover, the highest correlation between w_i and M_f (0.75%) was in I_NC_S, whereas the lowest correlation between w_i and M_f (0.38%) was in II_NC_S. Overall, w_i showed the highest correlation values with M_f in all drying runs, excluding II_NC_NS. Overall, ρ_b has the lowest correlation with M_f because ρ_b is naturally based on oven-dried weight and is independent of moisture level. Moreover, the volume change is negligible compared to weight change after kiln-drying, which further justifies the insubstantial correlation between ρ_b and M_f .

Table 5. The correlation between M_f and initial wood indices in nine drying runs (abbreviated names of the drying schedules are defined in Table 1).

Drying Schedule	Correlation between Wood Indices		
	M_i and M_f	w_i and M_f	ρ_b and M_f
UN	0.15	0.40	0.18
I_C_NS	0.62	0.74	0.28
I_NC_NS	0.54	0.61	0.29
II_NC_NS	0.22	0.59	0.60
I_C_S	0.45	0.61	0.29
I_NC_S	0.47	0.75	0.50
II_C_S	0.53	0.61	0.15
II_NC_S	0.25	0.38	0.12
II_C_NS	0.37	0.55	0.28

However, the correlation values in this study were considerably smaller than the findings of the former study [38]. In the former study, six drying batches underwent an identical drying schedule, while conditioning and post-storage were nonexistent. In contrast, this study included three drying schedules (with different M_{emc} at the final step) followed by conditioning and post-storage. These two post-drying treatments level out M_f variation and give grounds to the lower correlation between M_i and M_f .

3.2. Moisture Prediction by TreeNet

Figure 8 shows the relative importance (RI) of the inputs in the predictive model, indicating that w_i is the most remarkable parameter in this model (RI = 100), followed by the M_i (92.6%) and ρ_b (84.4%). The RI of drying schedule, post-storage, and conditioning were 63.3%, 45.0%, and 41.0%, respectively. This outcome shows that all the listed parameters considerably impact the model's performance, though they have different RI values. It is worth mentioning that these results are moderately different from the findings by Rahimi et al. [40], in which M_i was the most important input. This difference may stem from different drying schedules, applying post-drying treatments, or different timber dimensions (2" × 4" vs. 4" × 4").

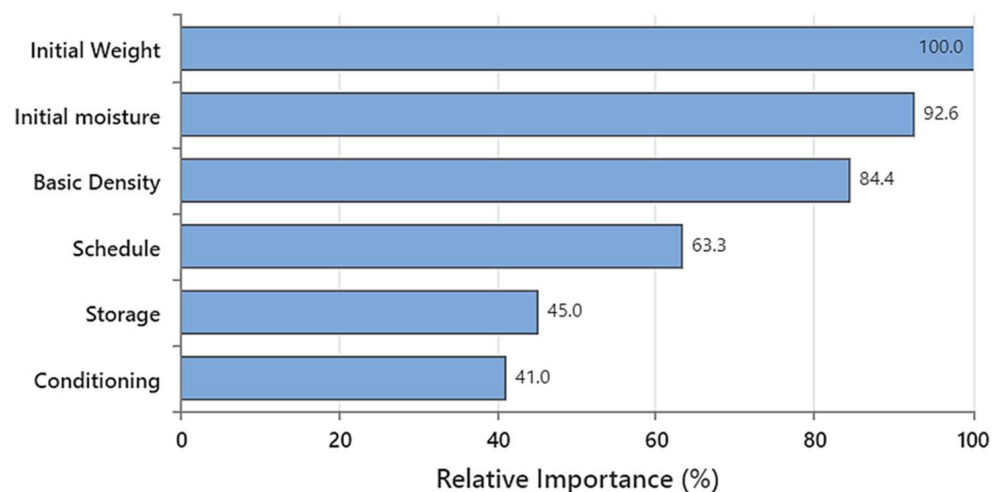
**Figure 8.** The relative importance of the inputs used to train the random forest approach for the M_f predictive model.

Table 6 lists the selected statistical parameters for the training and test datasets in the M_f predictive model. These results were based on the six predictors, including three wood attributes (M_i , w_i , and ρ_b) and three drying parameters (schedule, conditioning, and post-storage). The optimal performance (Figure 9) was achieved by having 550 trees in the model. The predictive model had an R^2 of 73.86% and 44.81% for the training and test, respectively.

Table 6. Model summary for predicting the M_f using TreeNet including six inputs.

Statistics	Training (%)	Test (%)
R-squared (R^2)	73.86	44.81
Root mean squared error (RMSE)	2.48	3.61
Mean squared error (MSE)	6.15	13.05
Mean absolute deviation (MAD)	1.68	2.43
Mean absolute percent error (MAPE)	0.12	0.17

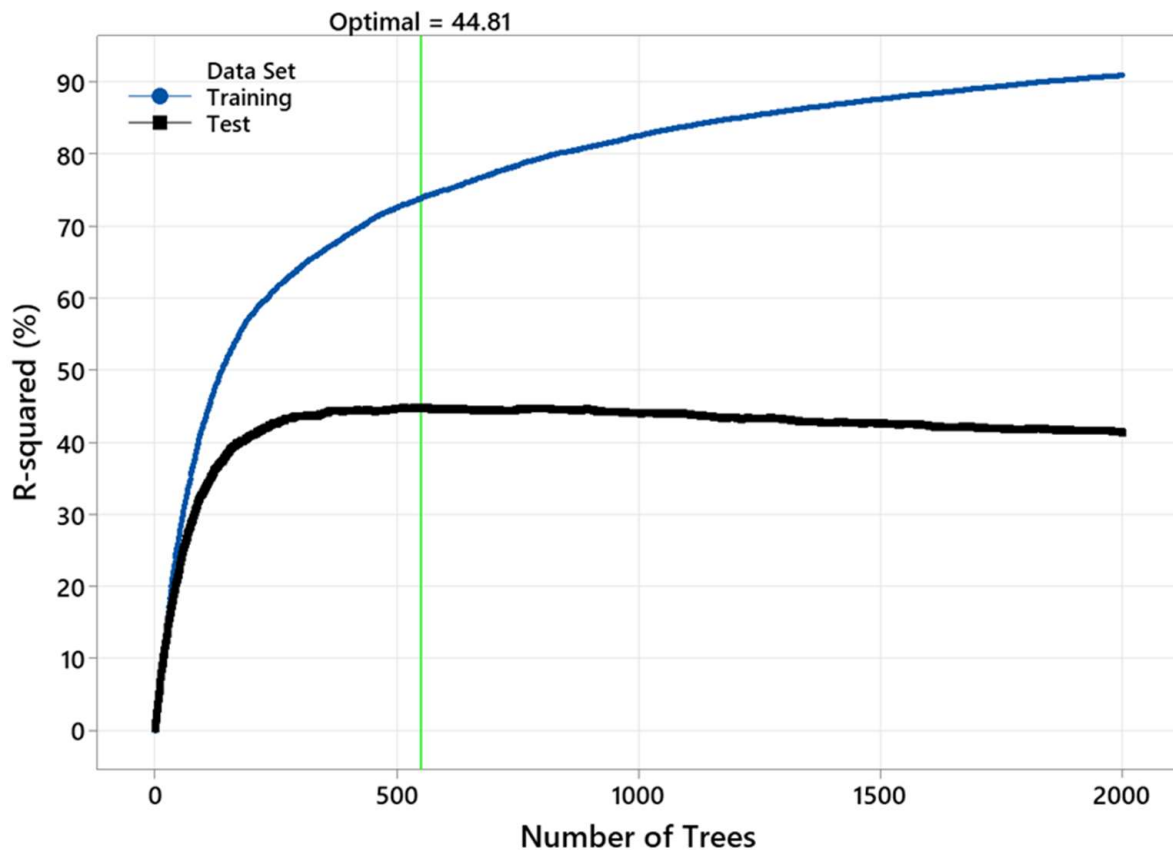


Figure 9. The variation in R^2 with the number of trees in the TreeNet model.

Figure 9 shows that the R^2 depends on the number of trees in the TreeNet model. This model had an unsatisfactory performance, with a low number of trees ($N < 250$). Comparing the training test results in Figure 9 discloses overfitting issues with the model. The actual (experimental) M_f versus the fitted (predicted) M_f is also shown in Figure 10.

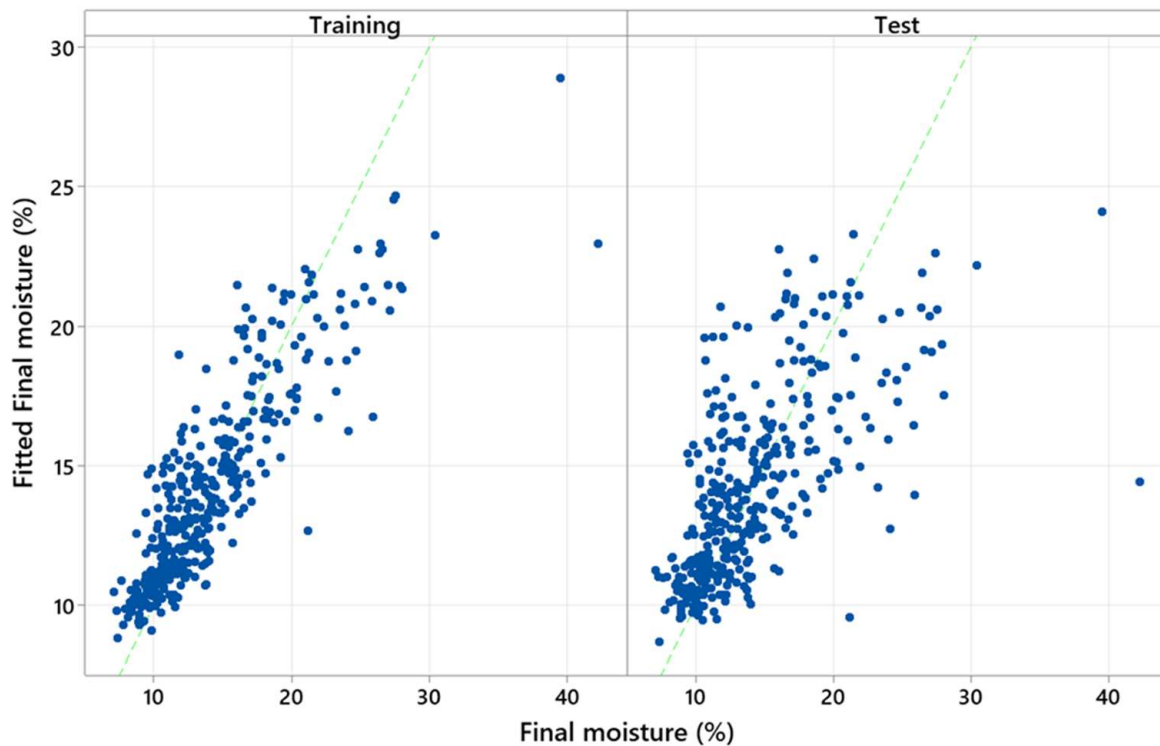


Figure 10. The actual M_f against the predicted M_f .

An additional study was performed to assess the role of the categorical parameters, including the drying schedule, conditioning, and post-storage, on the performance of the predictive model. Thus, another regression model was trained, using only three parameters (M_i , w_i , and ρ_b). Table 7 shows the model summary for this analysis. This model included 2000 grown trees with 214 optimal numbers of trees. The predictive model had an R^2 of 56.80% and 32.10% for the training and test, respectively. A comparison between the results of the two models (Tables 6 and 7) reveals that including the drying parameters improved the accuracy of the predictive model. Overall, the developed model failed to predict the M_f accurately. This failure is justified by the small sample size per drying run (42 boards) compared to the previous research (384 boards) [38]. Furthermore, applying post-drying treatments leveled off the moisture variation and slightly diluted the role of M_i in predicting M_f .

Table 7. Model summary for predicting the M_f using TreeNet including three inputs.

Statistics	Training (%)	Test (%)
R-squared (R^2)	56.80	32.10
Root mean squared error (RMSE)	3.19	4.00
Mean squared error (MSE)	10.17	16.04
Mean absolute deviation (MAD)	2.33	2.92
Mean absolute percent error (MAPE)	0.17	0.21

3.3. Moisture Classification

Since the regression approach failed to predict the M_f with acceptable accuracy, it was attempted to classify the M_f as having the input parameters and predict the chance of having over- or under-dried timber. This would be a crucial quality control task for drying processes. Accordingly, the classification was performed using TreeNet with the same assumption defined for the regression approach. Figure 11 illustrates the RI of the inputs in the predictive model for moisture classification. In this model, w_i is the most important parameter (RI = 100), followed by M_i (90.0%) and ρ_b (71.8%). The RI values of schedule,

post-storage, and conditioning were, in turn, 53.7%, 43.7%, and 32.7%, respectively. It is observed that the inputs have the same order in terms of relative importance for the moisture prediction (Figure 8) and moisture classification (Figure 11) models.

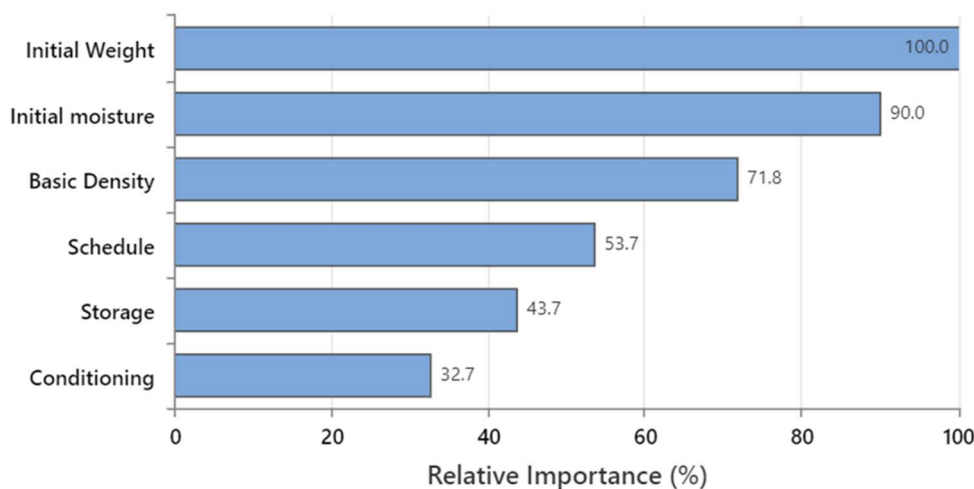


Figure 11. The relative importance of the inputs used to train the random forest approach for the M_f classifier model.

Table 8 lists the confusion matrix and the classification summary. The highest accuracy for the training and test data belonged to the over-dried (89.66%) and acceptable class (71.64%). Additionally, the lowest accuracy for the training and test data belonged to the acceptable (71.64%) and over-dried (58.62%) classes. Overall, the model could classify the wood with an accuracy of 76.19% during the training and 69.05% for the test data. Considering the small sample size, this is a promising performance that could be further enhanced by expanding the dataset.

Table 8. Confusion matrix and the summary of the classification with a random forest model.

Actual Class	Count	Predicted Training Class				Predicted Test Class			
		Over-Dried	Acceptable	Under-Dried	Correct (%)	Over-Dried	Acceptable	Under-Dried	Correct (%)
Over-dried	58	52	5	1	89.66	34	23	1	58.62
Acceptable	268	44	192	32	71.64	38	192	38	71.64
Under-dried	52	0	8	44	84.62	2	15	35	67.31
ALL	378	96	205	77	76.19	74	230	74	69.05

Table 9 documents the summary of the misclassification and error. This result indicates that, collectively, the error increased from the training data (23.81%) to the test data (30.95%) for all classes. Classifying over-dried timber had the best training result, with a 10.34% error, while acceptable class had the best test result with a 28.36% error.

Table 9. Summary of misclassification and error for random forest model.

Actual Class	Count	Predicted Training Class		Predicted Test Class	
		Misclassified	Error (%)	Misclassified	Error (%)
Over-dried	58	6	10.34	24	41.38
Acceptable	268	76	28.36	76	28.36
Under-dried	52	8	15.38	17	32.69
ALL	378	90	23.81	117	30.95

Overall, classification could categorize timber pieces into three classes based on their M_f with acceptable accuracy. This could be beneficial to wood manufacturing companies, as sawmills can apply this model to improve pre-and post-sorting strategies. The optimum breakpoints for the dry-sort-re-dry method could be accurately determined using the outcome of this classification approach. It is noteworthy that this research included some limitations, including relatively small sample size (42 boards per run) and single setpoint ($M_t = 12\%$). Therefore, future research should focus on a bigger sample size to improve the training and test performance of the model. Moreover, future studies should broaden the range of M_f moisture prediction by selecting multiple M_t for different drying runs. This study utilized the TreeNet gradient boosting model. Despite the proven effectiveness of tree-based ensemble models, future research can perform comparative studies to better reveal the performance of the selected model against other techniques, such as ANNs or support vector machines. While this research focused on M_f between timber pieces, future studies may have to characterize and model M_f within every single piece of timber (core and shells) [74] and casehardening [75]. Moreover, future studies may have to provide predictive and classifying models for drying defects, such as surface checks [76], internal checks (honeycombing) [77], and shape distortions [78]. Finally, future research should investigate the effectiveness of different NDE methods for the fast and reliable assessment of timber MC. Acoustic and ultrasound signals were shown to be sensitive to wood characteristics such as MC [79]. Additionally, the suitability of near-infrared (NIR) spectroscopy, as a widely used NDE method for wood characterization and monitoring [80–83], could be assessed for MC monitoring in kiln-dried timber at sawmills.

4. Conclusions

This research provided a holistic approach that considers selected wood indices and drying parameters in modeling moisture after kiln drying. Including the drying parameters in the model significantly improved the accuracy of the TreeNet, despite showing lower relative importance compared to the wood attributes. This finding emphasizes that a robust and accurate model should include not only wood attributes but also drying parameters. From a practical standpoint, w_i had the highest correlation with M_f among the input variables. This result was outstanding from a practical viewpoint, as weighing timber in sawmills is a fast and non-destructive test. The outcome of this research is an advanced step in optimizing drying schedules concerning final moisture variation. Classifying models are highly applicable to optimizing post-sorting strategies such as dry-sort-re-dry.

Author Contributions: Conceptualization: S.R., V.N. and S.A.; Methodology: S.R., V.N. and S.A.; Software and Analysis: F.S. and V.N.; Writing: S.R. and V.N.; Editing: S.R., V.N., S.A. and F.S. All authors have read and agreed to the published version of the manuscript.

Funding: This research received no external funding.

Institutional Review Board Statement: Not applicable.

Data Availability Statement: Not applicable.

Acknowledgments: The authors would like to thank Katrin Rohrbach and FPInnovations for their collaborations and support.

Conflicts of Interest: The authors declare no conflict of interest.

References

1. Glass, S.V.; Zelinka, S.L. Chapter 4: Moisture Relations and Physical Properties of Wood. In *Wood Handbook Wood as an Engineering Material. General Technical Report FPL-GTR-282*; U.S. Department of Agriculture, Forest Service, Forest Products Laboratory: Madison, WI, USA, 2021; 22p.
2. Fathi, H.; Kazemirad, S.; Nasir, V. Anondestructive guided wave propagation method for the characterization of moisture-dependent viscoelastic properties of wood materials. *Mater. Struct.* **2020**, *53*, 147. [[CrossRef](#)]

3. Herrera-Díaz, R.; Sepúlveda-Villaruel, V.; Pérez-Peña, N.; Salvo-Sepúlveda, L.; Salinas-Lira, C.; Llano-Ponte, R.; Ananías, R.A. Effect of wood drying and heat modification on some physical and mechanical properties of radiata pine. *Dry. Technol.* **2018**, *36*, 537–544. [CrossRef]
4. Lamrani, B.; Bekkioui, N.; Simo-Tagne, M.; Ndukwu, M.C. Recent progress in solar wood drying: An updated review. *Dry. Technol.* **2022**, 1–23. [CrossRef]
5. Haygreen, J.G.; Bowyer, J.L. *Forest Products and Wood Science, an Introduction*, 3rd ed.; Iowa State University Press: Ames, IA, USA, 1996; 484p.
6. Reeb, J.E. *Drying Wood. FOR-55*; University of Kentucky: Lexington, KY, USA; Cooperative Extension Service: Fairbanks, AK, USA, 1997; 8p.
7. Pang, S. Moisture content gradient in a softwood board during drying: Simulation from a 2-D model and measurement. *Wood Sci. Technol.* **1996**, *30*, 165–178. [CrossRef]
8. Perre, P. *Fundamental Wood Drying*; European COST: Nancy, France, 2007; 366p.
9. Simpson, W.T. *Dry Kiln Operator's Manual*; United States Department of Agriculture, Forest Service Forest Products Laboratory: Madison, WI, USA, 1991; 256p.
10. Esping, B. *Energy Saving in Wood Drying*; Wood Technology Report No. 12; Svenska Traforsknings Institute: Stockholm, Sweden, 1982. (In Swedish)
11. Bond, B.H.; Espinoza, O. A decade of improved lumber drying technology. *Curr. For. Rep.* **2016**, *2*, 106–118. [CrossRef]
12. Simpson, W.T. Drying wood: A review-part I. *Dry. Technol.* **1983**, *2*, 235–264. [CrossRef]
13. Keey, R.B.; Langrish, T.A.; Walker, J.C. *Kiln-Drying of Lumber*; Springer Science & Business Media: Berlin, Germany, 2000; 326p.
14. Rosen, H.N. Drying of Wood and Wood Products. In *Handbook of Industrial Drying*, 2nd ed.; Marcel Dekker: New York, NY, USA, 1995; pp. 899–921.
15. Shahverdi, M.; Oliveira, L.; Avramidis, S. Kiln-drying optimization for quality pacific coast hemlock lumber. *Dry. Technol.* **2017**, *35*, 1867–1873. [CrossRef]
16. Rohrbach, K.; Oliveira, L.; Avramidis, S. Drying schedule structure and subsequent post-drying equalisation effect on hemlock timber quality. *Int. Wood Prod. J.* **2014**, *5*, 55–64. [CrossRef]
17. Nogi, M.; Yamamoto, H.; Okuyama, T. Relaxation mechanism of residual stress inside logs by heat treatment: Choosing the heating time and temperature. *J. Wood Sci.* **2003**, *49*, 22–28. [CrossRef]
18. Coast Forest Products Association Coastal Products. Available online: <http://www.coast-forest.org/products/product-directory/species/> (accessed on 24 November 2018).
19. Wada, N.; Avramidis, S.; Oliveira, L.C. Internal moisture evolution in timbers exposed to ambient conditions following kiln drying. *Eur. J. Wood Prod.* **2014**, *72*, 377–384. [CrossRef]
20. Sackey, E.K.; Avramidis, S.; Oliveira, L.C. Exploratory Evaluation of Oscillation Drying for Thick Hemlock Timbers. *Holzforschung* **2004**, *58*, 428–433. [CrossRef]
21. Bradic, S.; Avramidis, S. Impact of Juvenile Wood on Hemlock Timber Drying Characteristics. *For. Prod. J.* **2007**, *57*, 53–59.
22. Berberovic, A.; Milota, M.R. Impact of wood variability on the drying rate at different moisture content levels. *For. Prod. J.* **2011**, *61*, 435–442. [CrossRef]
23. Elustondo, D.; Oliveira, L.; Ananias, R.A. Visual method to assess lumber sorting before drying. *Dry. Technol.* **2013**, *31*, 32–39. [CrossRef]
24. Watanabe, K.; Mansfield, S.D.; Avramidis, S. Application of near-infrared spectroscopy for moisture-based sorting of green hem-fir timber. *J. Wood Sci.* **2011**, *57*, 288–294. [CrossRef]
25. Aune, J.E. *Kiln Tests with Species and Moisture Content Sorted, 116 mm Square, Hem-Fir Merch Lumber*; Final Report Prepared for the Stability Work Group; ZAIRAI Lumber Partnership Ltd.: Vancouver, BC, Canada, 2000.
26. Yang, L.; Liu, H. Study of the collapse and recovery of Eucalyptus urophydis during conventional kiln drying. *Eur. J. Wood Prod.* **2021**, *79*, 129–137. [CrossRef]
27. Dawson, B.S.; Pearson, H.; Kimberley, M.O.; Davy, B.; Dickson, A.R. Effect of supercritical CO₂ treatment and kiln drying on collapse in *Eucalyptus nitens* wood. *Eur. J. Wood Prod.* **2020**, *78*, 209–217. [CrossRef]
28. Botter-Kuisch, H.P.; Van den Bulcke, J.; Baetens, J.M.; Van Acker, J. Cracking the code: Real-time monitoring of wood drying and the occurrence of cracks. *Wood Sci. Technol.* **2020**, *54*, 1029–1049. [CrossRef]
29. Suchomelová, P.; Trcala, M.; Tippner, J. Numerical simulations of coupled moisture and heat transfer in wood during kiln drying: Influence of material nonlinearity. *BioResources* **2019**, *14*, 9786–9805.
30. Kumar, S.; Kelkar, B.U.; Mishra, A.K.; Jena, S.K. Variability in physical properties of plantation-grown progenies of *Melia composita* and determination of a kiln-drying schedule. *J. For. Res.* **2018**, *29*, 1435–1442. [CrossRef]
31. Marier, P.; Gaudreault, J.; Noguier, T. Kiln drying operations scheduling with dynamic composition of loading patterns. *For. Prod. J.* **2021**, *71*, 101–110. [CrossRef]
32. Yin, Q.; Liu, H.H. Drying stress and strain of wood: A Review. *Appl. Sci.* **2021**, *11*, 5023. [CrossRef]
33. Watanabe, K.; Matsushita, Y.; Kobayashi, I.; Kuroda, N. Artificial neural network modeling for predicting final moisture content of individual Sugi (*Cryptomeria japonica*) samples during air-drying. *J. Wood Sci.* **2013**, *59*, 112–118. [CrossRef]
34. Chai, H.; Chen, X.; Cai, Y.; Zhao, J. Artificial neural network modeling for predicting wood moisture content in high frequency vacuum drying process. *Forests* **2018**, *10*, 16. [CrossRef]

35. Rabidin, Z.A.; Seng, G.K.; Wahab, M.J.A. Characteristics of timbers dried using kiln drying and radio frequency-vacuum drying systems. In *MATEC Web of Conferences*; EDP Sciences: Les Ulis, France, 2017; Volume 108, p. 10001. [[CrossRef](#)]
36. Liu, H.; Zhang, J.; Jiang, W.; Cai, Y. Characteristics of commercial-scale Radio-frequency/vacuum (RF/V) drying for hardwood lumber. *BioResources* **2019**, *14*, 6923–6935. [[CrossRef](#)]
37. Ozsahin, S.; Murat, M. Prediction of equilibrium moisture content and specific gravity of heat-treated wood by artificial neural networks. *Eur. J. Wood Prod.* **2018**, *76*, 563–572. [[CrossRef](#)]
38. Rahimi, S.; Avramidis, S. Predicting moisture content in kiln dried timbers using machine learning. *Eur. J. Wood. Prod.* **2022**, *80*, 681–692. [[CrossRef](#)]
39. Rahimi, S.; Nasir, V.; Avramidis, S.; Sassani, F. Wood moisture monitoring and classification in kiln-dried timber. *Struct. Control Health Monit.* **2022**, *29*, e2911. [[CrossRef](#)]
40. Rahimi, S.; Nasir, V.; Avramidis, S.; Sassani, F. Benchmarking moisture prediction in kiln-dried Pacific Coast hemlock wood. *Int. Wood Prod. J.* **2022**, *13*, 219–226. [[CrossRef](#)]
41. Rahimi, S.; Avramidis, S.; Lazarescu, C. Estimating moisture content variation in kiln dried Pacific coast hemlock. *Holzforschung* **2021**, *76*, 26–36. [[CrossRef](#)]
42. Nisgoski, S.; de Oliveira, A.A.; de Muñiz, G.I.B. Artificial neural network and SIMCA classification in some wood discrimination based on near-infrared. *Wood Sci. Technol.* **2017**, *51*, 929–942. [[CrossRef](#)]
43. Cui, X.; Wang, Q.; Zhao, Y.; Qiao, X.; Teng, G. Laser-induced breakdown spectroscopy (LIBS) for classification of wood species integrated with artificial neural network (ANN). *Appl. Phys. B* **2019**, *125*, 56. [[CrossRef](#)]
44. Bardak, S.; Tiryaki, S.; Nemli, G.; Aydın, A. Investigation and neural network prediction of wood bonding quality based on pressing conditions. *Int. J. Adhes. Adhes.* **2016**, *68*, 115–123. [[CrossRef](#)]
45. Bardak, S.; Tiryaki, S.; Bardak, T.; Aydın, A.Y.T.A.Ç. Predictive performance of artificial neural network and multiple linear regression models in predicting adhesive bonding strength of wood. *Strength Mater.* **2016**, *48*, 811–824. [[CrossRef](#)]
46. Ayanleye, S.; Nasir, V.; Avramidis, S.; Cool, J. Effect of wood surface roughness on prediction of structural timber properties by infrared spectroscopy using ANFIS, ANN and PLS regression. *Eur. J. Wood Prod.* **2021**, *79*, 101–115. [[CrossRef](#)]
47. Tiryaki, S.; Aydın, A. An artificial neural network model for predicting compression strength of heat-treated woods and comparison with a multiple linear regression model. *Constr. Build. Mater.* **2014**, *62*, 102–108. [[CrossRef](#)]
48. Tiryaki, S.; Malkoçoğlu, A.; Özşahin, Ş. Using artificial neural networks for modeling surface roughness of wood in machining process. *Constr. Build. Mater.* **2014**, *66*, 329–335. [[CrossRef](#)]
49. Dong, X.; Yu, Z.; Cao, W.; Shi, Y.; Ma, Q. A survey on ensemble learning. *Front. Comput. Sci.* **2020**, *14*, 241–258. [[CrossRef](#)]
50. Rohrbach, K. Schedule and Post-Drying Storage Effects on Western Hemlock Squares Quality. Master's Thesis, University of British Columbia, Vancouver, BC, Canada, 2008; p. 113.
51. Kollmann, F. *Technologie des Holzes und der Holzwerkstoffe, Zweiter Band*; Springer: Berlin/Heidelberg, Germany, 1955.
52. Skaar, C. *Water in Wood*; Syracuse University Press: Syracuse, NY, USA, 1972.
53. Hao, B.; Avramidis, S. Annual ring orientation effect and slope of grain in hemlock timber drying. *For. Prod. J.* **2004**, *54*, 41–49.
54. Hao, B.; Avramidis, S. Timber moisture class assessment in kiln drying. *J. Inst. Wood Sci.* **2006**, *17*, 121–133. [[CrossRef](#)]
55. Siau, J.F. *Wood: Influence of Moisture on Physical Properties*; Department of Wood Science and Forest Products, Virginia Polytechnic Institute and State University: Blacksburg, VA, USA, 1995; 227p.
56. Steinberg, D. CART: Classification and regression trees. In *The Top Ten Algorithms in Data Mining*; Wu, X., Kumar, V., Eds.; Taylor & Francis Group: New York, NY, USA, 2009; pp. 179–201.
57. van Blokland, J.; Nasir, V.; Cool, J.; Avramidis, S.; Adamopoulos, S. Machine learning-based prediction of surface checks and bending properties in weathered thermally modified timber. *Constr. Build. Mater.* **2021**, *307*, 124996. [[CrossRef](#)]
58. Breiman, L.; Friedman, J.H.; Olshen, R.A.; Stone, C.J. *Classification and Regression Trees*; Chapman & Hall/CRC: Boca Raton, FL, USA, 1984.
59. van Blokland, J.; Nasir, V.; Cool, J.; Avramidis, S.; Adamopoulos, S. Machine learning-based prediction of internal checks in weathered thermally modified timber. *Constr. Build. Mater.* **2021**, *281*, 122193. [[CrossRef](#)]
60. Nasir, V.; Fathi, H.; Kazemirad, S. Combined machine learning–wave propagation approach for monitoring timber mechanical properties under UV aging. *Struct. Health Monit.* **2021**, *20*, 2035–2053. [[CrossRef](#)]
61. Nasir, V.; Fathi, H.; Fallah, A.; Kazemirad, S.; Sassani, F.; Antov, P. Prediction of mechanical properties of artificially weathered wood by color change and machine learning. *Materials* **2021**, *14*, 6314. [[CrossRef](#)]
62. Nasir, V.; Parvari, Y.; Fathi, H.; Kazemirad, S.; Sassani, F. Identification of wood species and duration of exposure in weathered wood using guided wave propagation. *Wood Mater. Sci. Eng.* **2022**, 1–12. [[CrossRef](#)]
63. Grinsztajn, L.; Oyallon, E.; Varoquaux, G. Why do tree-based models still outperform deep learning on tabular data? *arXiv* **2022**, arXiv:2207.08815.
64. Liaw, A.; Wiener, M. Classification and regression by random Forest. *R News* **2002**, *2*, 18–22.
65. Schubert, M.; Luković, M.; Christen, H. Prediction of mechanical properties of wood fiber insulation boards as a function of machine and process parameters by random forest. *Wood Sci. Technol.* **2020**, *54*, 703–713. [[CrossRef](#)]
66. Nasir, V.; Kooshkbaghi, M.; Cool, J.; Sassani, F. Cutting tool temperature monitoring in circular sawing: Measurement and multi-sensor feature fusion-based prediction. *Int. J. Adv. Manufac. Technol.* **2021**, *112*, 2413–2424. [[CrossRef](#)]

67. Nasir, V.; Kooshkbaghi, M.; Cool, J. Sensor fusion and random forest modeling for identifying frozen and green wood during lumber manufacturing. *Manuf. Lett.* **2020**, *26*, 53–58. [[CrossRef](#)]
68. Modeler, S.P. *Introducing TreeNet Gradient-Boosting Machine*; Minitab, LLC: State College, PA, USA, 2019.
69. Sun, Y.; Lin, Q.; He, X.; Zhao, Y.; Dai, F.; Qiu, J.; Cao, Y. Wood species recognition with small data: A deep learning approach. *Int. J. Comput. Intell. Syst.* **2021**, *14*, 1451–1460. [[CrossRef](#)]
70. Zhuang, Z.; Liu, Y.; Ding, F.; Wang, Z. Online color classification system of solid wood flooring based on characteristic features. *Sensors* **2021**, *21*, 336. [[CrossRef](#)] [[PubMed](#)]
71. Carty, D.M.; Young, T.M.; Zaretzki, R.L.; Guess, F.M.; Petutschnigg, A. Predicting and correlating the strength properties of wood composite process parameters by use of boosted regression tree models. *For. Prod. J.* **2015**, *65*, 365–371. [[CrossRef](#)]
72. Nasir, V.; Dibaji, S.; Alaswad, K.; Cool, J. Tool wear monitoring by ensemble learning and sensor fusion using power, sound, vibration, and AE signals. *Manuf. Lett.* **2021**, *30*, 32–38. [[CrossRef](#)]
73. Fathi, H.; Nasir, V.; Kazemirad, S. Prediction of the mechanical properties of wood using guided wave propagation and machine learning. *Const. Build. Mater.* **2020**, *262*, 120848. [[CrossRef](#)]
74. McMillen, J.M. *Stresses in Wood during Drying*; U.S. Department of Agriculture, Forest Service, Forest Products Laboratory: Madison, WI, USA, 1958; Volume 1652, 174p.
75. Diawanich, P.; Tomad, S.; Matan, N.; Kyokong, B. Novel assessment of casehardening in kiln-dried lumber. *Wood Sci. Technol.* **2012**, *46*, 101–114. [[CrossRef](#)]
76. Denig, J.; Wengert, E.M.; Simpson, W.T. *Drying Hardwood Lumber*; Gen. Tech. Rep. FPL-GTR-118; U.S. Department of Agriculture, Forest Service, Forest Products Laboratory: Madison, WI, USA, 2000; 138p.
77. Rahimi, S.; Faezipour, M.; Tarmian, A. Drying of internal-check prone poplar lumber using three different conventional kiln drying schedules. *J. Indian Acad. Wood Sci.* **2011**, *8*, 6–10. [[CrossRef](#)]
78. Pratt, G.H. *Timber Drying Manual*; Building Research Establishment: Buckinghamshire, UK, 1974; 152p.
79. Nasir, V.; Ayanleye, S.; Kazemirad, S.; Sassani, F.; Adamopoulos, S. Acoustic emission monitoring of wood materials and timber structures: A critical review. *Const. Build. Mater.* **2022**, *350*, 128877. [[CrossRef](#)]
80. Leblon, B.; Adedipe, O.; Hans, G.; Haddadi, A.; Tsuchikawa, S.; Burger, J.; Stirling, R.; Pirouz, Z.; Groves, K.; Nader, J.; et al. A review of near-infrared spectroscopy for monitoring moisture content and density of solid wood. *For. Chron.* **2013**, *89*, 595–606. [[CrossRef](#)]
81. Tsuchikawa, S.; Kobori, H. A review of recent application of near infrared spectroscopy to wood science and technology. *J. Wood Sci.* **2013**, *61*, 213–220. [[CrossRef](#)]
82. Tsuchikawa, S. A review of recent near infrared research for wood and paper. *Appl. Spectrosc. Rev.* **2007**, *42*, 43–71. [[CrossRef](#)]
83. Tsuchikawa, S.; Schwanninger, M. A review of recent near-infrared research for wood and paper (Part 2). *Appl. Spectrosc. Rev.* **2013**, *48*, 560–587. [[CrossRef](#)]

Disclaimer/Publisher’s Note: The statements, opinions and data contained in all publications are solely those of the individual author(s) and contributor(s) and not of MDPI and/or the editor(s). MDPI and/or the editor(s) disclaim responsibility for any injury to people or property resulting from any ideas, methods, instructions or products referred to in the content.